Biochemical Pharmacology 80 (2010) 308–315

Contents lists available at ScienceDirect

Biochemical Pharmacology

journal homepage: www.elsevier.com/locate/biochempharm

Metabolism of short-chain ceramide by human cancer cells—Implications for therapeutic approaches

Jacqueline V. Chapman [a], Valérie Gouazé-Andersson [a], Maria C. Messner [a], Margaret Flowers [a], Ramin Karimi [a], Mark Kester [b], Brian M. Barth [b], Xin Liu [b], Yong-Yu Liu [c], Armando E. Giuliano [a], Myles C. Cabot [a,*]

[a] John Wayne Cancer Institute at Saint John's Health Center, Department of Experimental Therapeutics, 2200 Santa Monica Boulevard, Santa Monica, CA 90404, USA
[b] Penn State Hershey Cancer Center, Hershey, PA, USA
[c] Department of Basic Pharmaceutical Sciences, University Louisiana at Monroe, Monroe, LA, USA

ARTICLE INFO

Article history:
Received 20 January 2010
Accepted 1 April 2010

Keywords:
Ceramide
Glucosylceramide
Cancer cells
Tamoxifen

ABSTRACT

Due to recent use of short-chain ceramides in preclinical studies, we characterized C6-ceramide metabolism in cancer cell lines and assessed metabolic junctures for enhancing efficacy. MDA-MB-231 breast cancer cells decreased the amount of C6-ceramide metabolized to C6-sphingomyelin (C6-SM) and increased the amount metabolized to C6-glucosylceramide (C6-GC) in response to increasing concentrations. A similar trend was seen in DU-145 (prostate cancer), PANC-1 (pancreatic cancer), and LoVo (colorectal cancer) cells. KG-1 leukemia cells favored C6-SM synthesis at low (0.6 μM) and high-dose (12 μM) C6-ceramide. Partnering C6-ceramide with tamoxifen, a P-glycoprotein antagonist that impedes ceramide glycosylation, was an effective regimen for enhancing cytotoxicity in cells. Experiments to assess the mechanism of cell death using KG-1 cells showed that tamoxifen inhibited synthesis of C6-GC and C6-SM from C6-ceramide by 80% and 50%, respectively, which was accompanied by enhanced apoptosis. Radiolabeling of KG-1 cells with [^{3}H]palmitic acid produced a 2-fold increase in ^{3}H-long-chain ceramides when unlabeled C6-ceramide was added and a 9-fold increase when C6-ceramide and tamoxifen were added. The increase in ^{3}H-palmitate radiolabeling of long-chain ceramides was blocked by inclusion of a ceramide synthase inhibitor; however, inhibiting synthesis of long-chain ceramide did not rescue cells. These studies show that tamoxifen enhances the apoptotic effects of C6-ceramide. The proposed mechanism involves blocking short-chain ceramide anabolism to favor hydrolysis and generation of sphingosine. We propose that use of tamoxifen and other P-glycoprotein antagonists can be an effective means for enhancing cytotoxic potential of short-chain ceramides in the treatment of cancer.

1. Introduction

Previous studies with chemotherapy-sensitive and chemotherapy-resistant cancer cells demonstrated a clear distinction in cerebroside content as shown by the accumulation of a glycosylated form of ceramide, glucosylceramide (GC) [1]. This lipid is characteristic to drug-resistant cancer cells derived from breast, ovary, melanoma, colon, and leukemia [2–5]. Investigations on the mechanism underlying the GC surplus in chemoresistant cancer cells showed that exposure of wild-type cancer cells to doxorubicin produced an increase in intracellular ceramide and cell death attributed to apoptosis, whereas in chemoresistant cells treated similarly, the ceramide generated was converted to GC and the cytotoxic response was diminished [6]. This indicates that drug-resistant cells have enhanced capacity to metabolize ceramide through glucosylceramide synthase (GCS), and indeed GCS has been shown pivotal in cancer cell response to ceramide-generating anticancer agents [7,8], reviewed in Cabot [9].

Studies assessing short-chain ceramide cytotoxicity have shown that wild-type cancer cells were sensitive to C6-ceramide whereas some drug-resistant cancer cell lines were unresponsive [10]; this resistance has been linked to the higher rates of ceramide glycosylation associated with the multidrug-resistant phenotype. Such findings suggest a role for multidrug resistance proteins in addition to the role of GCS in C6-ceramide metabolism. Few in-depth studies have been conducted examining C6-ceramide metabolism in cancer cells.

The role of ceramide metabolism in regulating tumor cell response to chemotherapy has been demonstrated by GCS over-expression, wherein GCS transfectants became resistant to doxorubicin, ceramide analogs, and tumor necrosis factor-α (TNF-α), compared to mock-transfectants [7,11]. Introduction of GCS

* Corresponding author. Tel.: +1 310 998 3924; fax: +1 310 582 7325.
E-mail address: cabot@jwci.org (M.C. Cabot).

0006-2952/$ – see front matter © 2010 Elsevier Inc. All rights reserved.
doi:10.1016/j.bcp.2010.04.001

antisense into multidrug-resistant cancer cells and tumors, a reverse tactic heightened chemotherapy sensitivity [8,12]. Other studies have shown that GCS antisense-transfected multidrug-resistant cells were nearly devoid of MDR1/P-glycoprotein (P-gp), compared to the parent cells [13], an indication that P-gp, GCS, and GC are interrelated.

Interestingly, a number of P-gp antagonists including tamoxifen have been shown to diminish GC levels in multidrug-resistant cancer cells [14]. For example, clinically relevant concentrations of tamoxifen, verapamil, and cyclosporin A, markedly decreased GC levels in NCI/ADR-RES cells [15]. Toremifene, an anti-estrogen with chemistry and pharmacology similar to tamoxifen, has been shown equally effective [10]. These studies suggest that P-gp-targeted agents act not only by blocking cellular drug efflux but also by modifying ceramide metabolism.

Results from studies using chemical agents that are specific inhibitors of GCS also demonstrated that blocking ceramide anabolism increases cytotoxic response to anticancer agents. For example, PPMP (1-phenyl-2-palmitoylamino-3-morpholino-1-propanol) [16] sensitizes NCI/ADR-RES cells to doxorubicin [15] and neuroblastoma cells to taxol and vincristine [17]. Using C6-ceramide, Spinedi et al. [18] showed that 1-phenyl-2-decanoylamino-3-morpholino-1-propanol (PDMP), a chemical cousin of PPMP, suppressed GC synthesis and potentiated the apoptotic effect of short-chain C6-ceramide in neuroepithelioma, again suggesting that cellular GC synthesis is one mechanism to escape ceramide-induced apoptosis.

Recent interest in the ceramide field has sparked a number of clinical translational studies. For example, the ceramide-generating properties of 4-HPR (fenretinide), are being evaluated in a phase II study of recurrent ovarian cancer [19], and in the realm of nanotechnology, C6-ceramide nanoliposomes are being evaluated as a neoplastic-selective agent [20]. Several recent reviews have been written on therapeutic targeting of ceramide pathways as a strategy against cancer [21–25]. In light of current interest and the application of ceramide-based therapies in the form of ceramide-generating drugs and short-chain ceramide formulations, knowledge of ceramide metabolism at the cellular level is essential to improve efficacy. The present investigation was conducted to characterize the cellular fate of C6-ceramide and to test whether P-gp antagonists, which attenuate ceramide glycosylation, can be employed as effective enhancers of cytotoxicity.

2. Materials and methods

2.1. Cell culture

The following human cell lines were obtained from the American Type Culture Collection (Manassas, VA), MDA-MB-231 (breast cancer), DU-145 (prostate cancer), PANC-1 (pancreatic cancer), LoVo (colorectal cancer), and KG-1 (acute myeloid leukemia). MDA-MB-231, LoVo, and PANC-1 cells were propagated in RPMI-1640 medium, and DU-145 and KG-1 cells were grown in minimum essential medium (Eagle) and Iscove's modified Dulbecco's medium, respectively. All growth media (Invitrogen Corp, Carlsbad, CA) contained 10% fetal bovine serum (HyClone, Logan, UT, and Atlanta Biological, Atlanta, GA), 50 units/ml penicillin, 50 μg/ml streptomycin, and 584 mg/l L-glutamine (Invitrogen Corp, Carlsbad, CA). Cells were grown in a humidified atmosphere, 95% air, 5% CO_2 at 37 °C and subcultured at confluence using Gibco 0.05% trypsin/0.53 mM EDTA solution (Invitrogen Corp, Carlsbad, CA).

2.2. Cell viability assays

Assays were performed as described previously [7]. Generally, MDA-MB-231 cells (3000 cells/well) and LoVo and KG-1 cells (10,000 cells/well) were seeded in 96-well plates (perimeter wells contained water) in 0.1 ml complete medium and cultured at 37 °C for 24 h before adding agents. C6-Ceramide (*N*-hexanoyl-D-*erythro*-sphingosine) was from Avanti Polar Lipids, Alabaster, AL. Verapamil-HCl, cyclosporin A, and myriocin, purchased from Sigma Chemical Co, St. Louis, MO, were dissolved in 100% ethanol, stored as stock solutions (5–20 mM) at −20 °C, and diluted into 37 °C culture medium just prior to use. Ethanol was also used as a vehicle for C6-ceramide. Treatment media were made fresh each time. After addition of agents, cells were cultured at 37 °C for 72 h unless otherwise stated, and viability was determined using Promega's CellTiter 96 Aqueous One Solution cell proliferation assay kit (MTS) (Promega, Milwaukee, WI). Absorbance at 490 nm was recorded using a Microplate Fluorescent Reader FL600, BIO-TEK Instruments (Winooski, VT).

2.3. Flow cytometry analysis

Cells treated in Falcon™ 6-well plates (BD Biosciences, San Jose, CA) were prepared and stained using the FITC Annexin V Apoptosis Detection Kit (BD Biosciences, San Jose, CA) according to the manufacture's instructions. Briefly, cells were washed twice in PBS (Mediatech Inc, Manassas, VA) and approximately 10^5 cells were stained with FITC Annexin V and propidium iodide in 1X binding buffer for 15 min at room temperature in the dark. Cells were processed on a BD FACS Calibur equipped with a blue argon laser (488 nm), and data were analyzed using CellQuest software.

2.4. Lipid analysis – [^{14}C]C6-ceramide metabolism

[^{14}C]C6-ceramide (*N*[^{14}C]hexanoyl-sphingosine) was a gift from Dr. A. Bielwaska, Medical University of Southern Carolina, Charleston, and was synthesized as described previously [26]. The radiospecific activity of [^{14}C]C6-ceramide upon preparative TLC purification was 135,118 dpm/nmol. In some experiments in which the amount of C6-ceramide was increased, the amount of [^{14}C]C6-ceramide was kept constant and unlabeled C6-ceramide was increased; this was taken into account when calculating radiospecific activities. Details are given in the figure legends. To assess metabolism, cells were seeded in 6-well plates (5×10^5 to 1.0×10^6/well, see figure legends for details) and supplemented with [^{14}C]C6-ceramide the following day for 24 h. Lipids in the total lipid extracts were analyzed by TLC. [^{14}C]C6-ceramide, [^{14}C]C6-GC, [^{14}C]C6-lactosylceramide, and [^{14}C]C6-sphingomyelin (SM) were resolved in a solvent system containing chloroform/methanol/acetic acid/water (65:25:2:2, v/v), or a slight variation thereof, in filter paper-lined chromatography tanks. An alternate solvent was also used containing chloroform/methanol/ammonium hydroxide (65:35:4, v/v). Commercial lipid standards were co-chromatographed. Lipids were visualized in iodine vapor, and the lipids of interest were scraped into plastic mini-scintillation vials (6 ml) (Research Products International, Mt. Prospect, IL) containing 0.5 ml of water. EcoLume scintillation counting fluid (MP Biomedicals, Santa Ana, CA) (4 ml) was added, the samples were vortex mixed. Radioactivity was determined by liquid scintillation counting (LSC) (Beckman LS 6500, Brea, CA).

2.5. Lipid analysis – [^{3}H]palmitic acid radiolabeling

To determine the effect of unlabeled C6-ceramide and other agents on the metabolism of long-chain ceramide, cells were seeded in 6-well plates and the following day exposed to C6-ceramide in medium containing 1.0 μCi/ml [9,10-^{3}H]palmitic acid, 40–60 Ci/mmol (American Radiolabeled Chemicals, St. Louis, MO) for 24 h. Long-chain ^{3}H-ceramides were resolved in the total cell lipid extracts by TLC in a solvent system containing chloroform/

acetic acid (90:10, v/v). Solvents, HPLC grade, were purchased from Fisher Scientific, Los Angeles, CA, and MP Biomedicals, Santa Ana, CA. Commercial brain ceramides (Avanti Polar Lipids, Inc) and monooleoylglycerol (Nu Chek Prep, Alysian, MN) were co-chromatographed, the latter because monoacylglycerols run just below ceramide. Tritiated ceramide was quantitated as described in Section 2.4.

2.6. Western blotting

P-gp detection by Western blot was conducted as previously described [13]. Pre-cast 4–20% gradient SDS-PAGE gels were used (Invitrogen Corp, Carlsbad, CA). Murine monoclonal antibody against human P-gp was purchased from EMD Chemicals (Newark, NJ), formerly Calbiochem.

2.7. Data computation

C6-ceramide and long-chain ^{3}H-ceramide metabolism experiments were conducted in triplicate and data represent the average ± standard deviation (error bars). Cell viability data represent the average ± standard deviation, $n = 6$. Lipid metabolism and cell viability results are representative of 2–3 experiments. Drug-induced cytotoxic synergy was calculated using Calcusyn software from BioSoft (Great Shelford, Cambridge, United Kingdom). By this method, a combination index (CI) equal to 1.0 indicates additive effects, 0.85–0.7 indicates moderate synergy, and 0.7–0.3 indicates synergism. A CI of 0.3–0.1 indicates strong synergism.

3. Results

3.1. C6-ceramide metabolism and cytotoxicity

The metabolic fate of C6-ceramide in MDA-MB-231 cells was investigated as a function of increasing concentration using [^{14}C]C6-ceramide. The data in Fig. 1 demonstrate the versatility of MDA-MB-231 cells to metabolize C6-ceramide. At low dose, cells converted C6-ceramide primarily to C6-SM. For example, at 0.6 μM, >80% of cellular ^{14}C was present in the form of C6-SM, 4% as C6-GC, nil as lactosylceramide (LacCer), and 13% as C6-ceramide. At high-dose C6-ceramide (10 μM), the majority of radioactivity was channeled into C6-GC (75%), whereas SM synthesis accounted for only 15% of radioactivity. This experiment demonstrates that at challenge doses of C6-ceramide, MDA-MB-231 cells remove ceramide primarily by glycosylation via GCS, whereas lower doses are channeled into SM via SM synthase. A third route of metabolism, that of hydrolysis, is discussed in Sections 3.5 and 3.6.

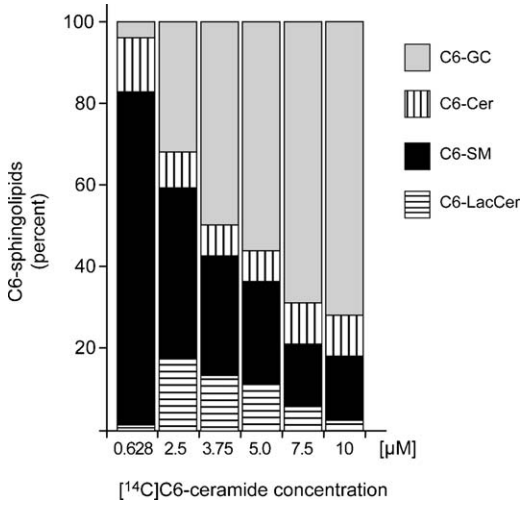

Fig. 1. Influence of C6-ceramide concentration on metabolic fate in MDA-MB-231 breast cancer cells. Cells (500,000/well) were seeded in 6-well plates and the following day exposed to [^{14}C]C6-ceramide at the concentration indicated. Radioactivity was held constant (84,500 dpm/ml) and mass was increased by addition of nonradioactive C6-ceramide. After 24 h exposure, total lipids were extracted and analyzed by TLC. Data obtained from single cultures at each C6-ceramide concentration represent percent of each of the four lipid classes based on pmol formed (calculated using the radiospecific activity at each concentration). Short-chain sphingolipids were discernable from long-chain counterparts by TLC. The experiment was repeated twice, and similar results were obtained. LacCer, lactosylceramide.

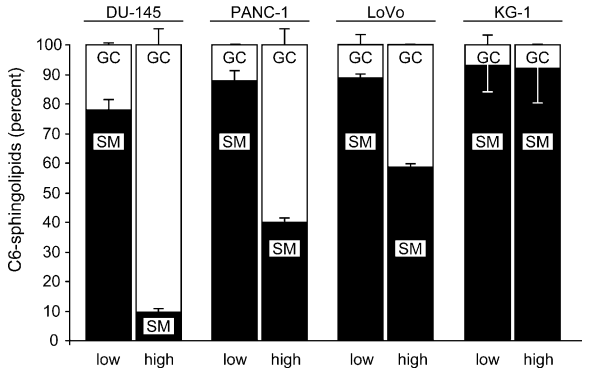

Fig. 2. Effect of low- and high-dose C6-ceramide on C6-GC and C6-SM formation in human cancer cell lines. Cells were seeded in 6-well plates at 750,000/well except for KG-1 (1.5×10^{6}/well) and incubated the following day with low-dose (0.6 μM) and high-dose (12.6 μM) [^{14}C]C6-ceramide for 24 h. Cell lipids were extracted and analyzed by TLC. Data represent percent in each lipid class calculated using the radiospecific activity at each dose. Uptake by DU-145 and PANC-1 cells was as follows: DU-145, low- and high-dose, 6.8% and 17.3%, respectively; PANC-1, low- and high-dose, 8.6% and 11.7%, respectively. Uptake by LoVo and KG-1 cells was as follows: LoVo, low- and high-dose, 7.3% and 4.6%, respectively; KG-1, low- and high-dose, 4.9% and 6.2%, respectively.

To determine whether converting high-dose C6-ceramide to C6-GC was characteristic in other cancer cell types, we evaluated DU-145 prostate cancer cells, PANC-1 pancreatic cancer cells, LoVo colorectal cancer cells, and KG-1 AML leukemia cells. The data in Fig. 2 show that DU-145 and PANC-1 cells, like MDA-MB-231 cells, favor synthesis of C6-SM at low-dose and C6-GC at high-dose C6-ceramide; however, in LoVo cells, the majority of radioactivity with high-dose C6-ceramide (60%) was in the C6-SM fraction. In KG-1 cells, C6-SM synthesis was the predominant metabolic pathway with both low and high-dose C6-ceramide.

We compared the relative levels of natural ceramide and GC by steady state [^{3}H]palmitic acid radiolabeling (24 h) in MDA-MB-231, LoVo, and KG-1 cells. In MDA-MB-231 cells, ceramide and GC accounted for 0.4% and 2.2% of total lipid tritium, respectively. In LoVo cells ceramide and GC comprised of 0.4% and 1.0% of total lipid, respectively, and in KG-1 cells, ceramide and GC accounted for 0.7% and 0.7% total lipids, respectively.

3.2. Effect of tamoxifen on C6-ceramide metabolism and cytotoxicity in MDA-MB-231 breast cancer cells

Tamoxifen, a front-line antiestrogen and P-gp antagonist, and other P-gp antagonists such as verapamil and cyclosporine A, block formation of natural GC in multidrug-resistant cancer cells [15]. One objective of the present study was to determine whether tamoxifen would inhibit C6-GC synthesis from C6-ceramide and establish whether tamoxifen, like the GCS inhibitor PPMP, would enhance C6-ceramide cytotoxicity. Tamoxifen inhibited C6-GC synthesis from C6-ceramide by 72% (Fig. 3A). Tamoxifen had little effect on C6-SM synthesis (Fig. 3B). We then determined whether tamoxifen would enhance C6-ceramide cytotoxicity. The photomicrographs (Fig. 3C) illustrate that C6-ceramide partnered with

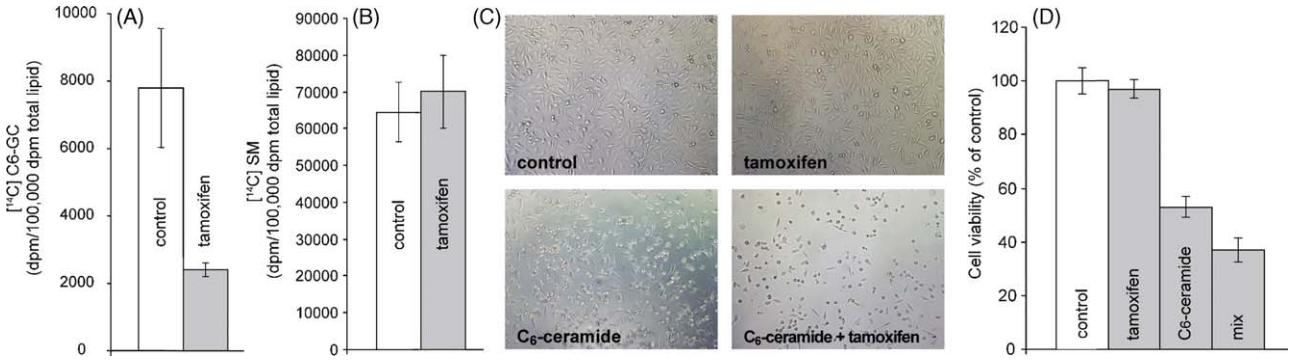

Fig. 3. The influence of tamoxifen on C6-ceramide metabolism and cytotoxicity in MDA-MB-231 cells. (A) Tamoxifen influence on C6-GC synthesis. (B) Influence of tamoxifen on C6-SM synthesis. Cells in 6-well plates were grown with 0.7 μM [^{14}C]C6-ceramide for 24 h; C6-GC and C6-SM were quantified by TLC of the total lipid extracts. (C) Cell morphology and cell population density photomicrographs. Cells were grown with C6-ceramide (10 μM), tamoxifen (10 μM), or the combination for 24 h. (D) Cell viability by MTS assay. Viability was measured after 24 h exposure to the indicated agents; concentrations as in C. (D) CI = 0.8 (moderate synergism). CI = 0.7 (synergism) for C6-ceramide 5 μM + tamoxifen 10 μM (data not shown).

tamoxifen was more cytotoxic than either single agent. Tamoxifen exposure imparted only slight morphological changes such as vacuolization (Fig. 3C), and it was not cytotoxic as shown by cell viability assays (Fig. 3D). Exposure of cells to 10 μM C6-ceramide, a dose that was primarily metabolized to C6-GC in MDA-MB-231 cells (see Fig. 1), elicited cell rounding, diminished cell growth (Fig. 3C), and decreased cell viability (55% of control) (Fig. 3D). In contrast, the C6-ceramide/tamoxifen regimen greatly diminished cell number, increased cell rounding (Fig. 3C), and decreased cell viability to 37% of control (Fig. 3D).

3.3. Effect of tamoxifen on C6-ceramide metabolism and cytotoxicity in LoVo colorectal cancer cells

Tamoxifen inhibited C6-GC synthesis from C6-ceramide by 90% in LoVo cells (Fig. 4A). This was accompanied by a 50% increase in [^{14}C]C6-SM (Fig. 4B). The influence of tamoxifen on C6-ceramide cytotoxicity in LoVo cells was striking. Whereas C6-ceramide and tamoxifen at 5 μM imparted only slight changes in viability, 92% and 103% of control respectively, the mixture brought cell viability to 39% of control (Fig. 4C). With 5 μM C6-ceramide and 10 μM tamoxifen, cell viability dipped to 17% of control.

3.4. Effect of tamoxifen on C6-ceramide metabolism and cytotoxicity in KG-1 leukemia cells

Leukemia cells, which grow in suspension, metabolized C6-ceramide predominantly to C6-SM (see Fig. 2). Tamoxifen inhibited C6-GC synthesis by >80% in KG-1 cells (Fig. 5A). Tamoxifen also inhibited C6-SM formation by nearly 50% (Fig. 5B). Thus, tamoxifen prevented metabolism of C6-ceramide along two major anabolic routes, C6-GC and C6-SM. Cell viability in response to C6-ceramide and tamoxifen was measured by MTS and flow cytometry. As shown in Fig. 5C, whereas C6-ceramide and tamoxifen imparted similar decreases in viability (approximately 30%) the combination brought cell viability to zero. Annexin V binding and propidium iodide staining confirmed that C6-ceramide and tamoxifen separately were not cytotoxic; however, the mixture produced a large increase in the population of cells that stained with propidium iodide (Fig. 5D).

3.5. C6-ceramide hydrolysis in MDA-MB-231, LoVo, and KG-1 cells

The above experiments characterized C6-ceramide conversion to higher sphingolipids but did not take into account C6-ceramide hydrolysis. Ogretmen et al. [27] reported that short-chain

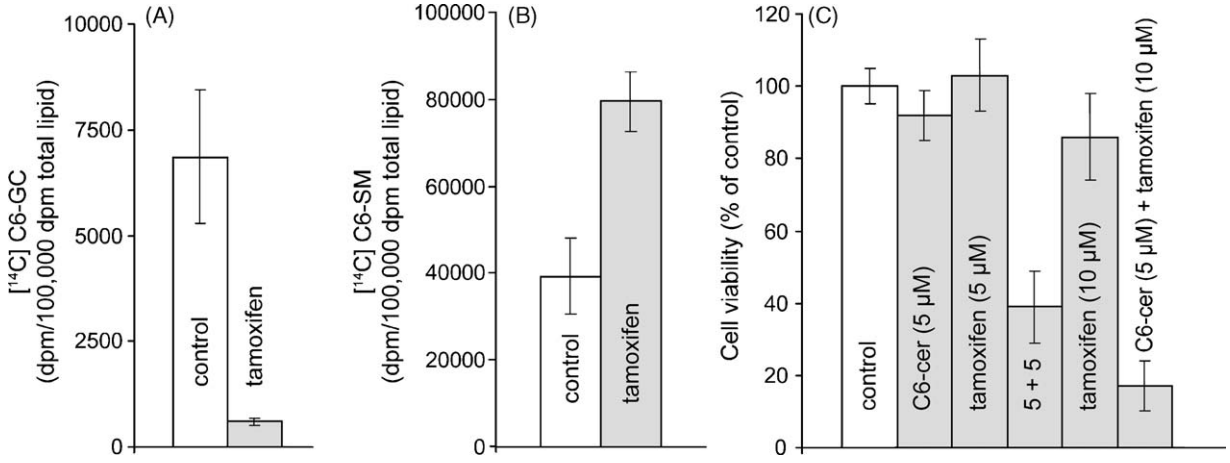

Fig. 4. The effect of tamoxifen on C6-ceramide metabolism and cytotoxicity in human colorectal cancer cells, LoVo. (A, B) Effect of tamoxifen on metabolic fate of C6-ceramide. Cells were seeded in 6-well plates and exposed the following day to [^{14}C]C6-ceramide (5 μM) in the absence and presence of tamoxifen (10 μM) for 24 h. Cell lipids were extracted and analyzed by TLC. (C) Effect of C6-ceramide and tamoxifen on cell viability. Cells were seeded in 96-well plates (10,000 cells/well) and exposed the following day to the agents indicated for 72 h. Viability was measured by MTS assay. 5 + 5, equimolar amounts of C6-ceramide and tamoxifen. CI = 0.19 (strong synergism), 5 μM C6-ceramide + 10 μM tamoxifen. CI = 0.10 (strong synergism).

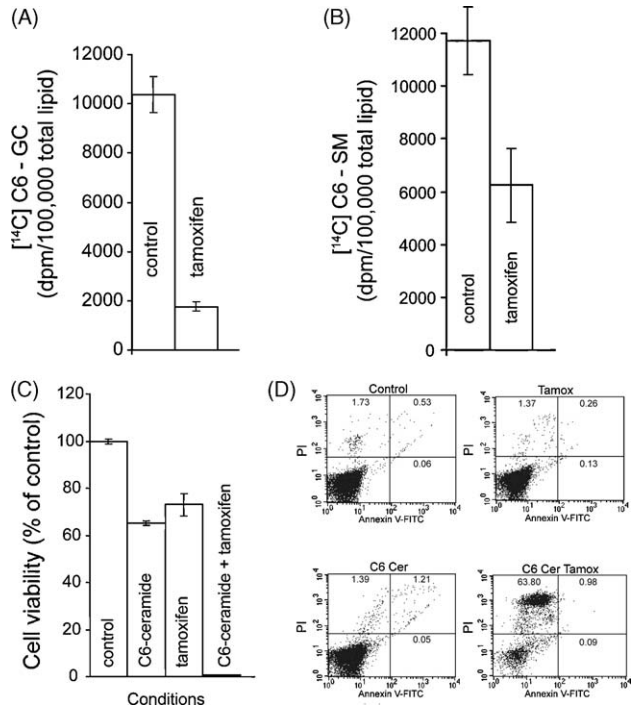

Fig. 5. Effect of tamoxifen on C6-ceramide metabolism and cytotoxicity in KG-1 human leukemia cells. (A, B) Effect of tamoxifen on C6-ceramide conversion to C6-GC and C6-SM. Cells (1×10^6/well) were seeded in 6-well plates and treated the following day with 12 μM [^{14}C]C6-ceramide (84,500 dpm/well) in the absence and presence of tamoxifen (5 μM) for 24 h. Total lipids were extracted and analyzed for [^{14}C]C6-GC and [^{14}C]C6-SM by TLC and LSC. (C) Cell viability by MTS assay. Cells (10,000/well) were seeded into 96-well plates and the following day treated with C6-ceramide (10 μM) and tamoxifen (5 μM) for 72 h. (D) Annexin V binding and propidium iodide staining. KG-1 cells seeded into 6-cm dishes were treated as in C, and after 24 h cells analyzed by flow cytometry as described in Section 2. (C) CI = 0.6 (synergism); CI = 1.0 (additive) for 5 μM C6-ceramide, plus 5 μM tamoxifen (data not shown).

ceramide was hydrolyzed by A549 human lung adenocarcinoma cells and the resultant long-chain sphingosine base was utilized by ceramide synthase for synthesis of long-chain ceramide. To determine whether this occurred in the various cancer cell lines, we analyzed the influence of unlabeled C6-ceramide on incorporation of [^{3}H]palmitic acid into long-chain ceramides. As shown in Fig. 6, the presence of unlabeled C6-ceramide in the culture medium increased the incorporation of [^{3}H]palmitic acid into long-chain ceramide by 2.1-, 1.3-, 3.2-, and 4.1-fold in MDA-MB-231, LoVo, KG-1, and PANC-1 cells, respectively. In KG-1 cells, based on cpm/100,000 cpmcpm total lipid tritium, ceramides increased from 0.65% to 2.1% of total lipid.

3.6. Effect of tamoxifen on C6-ceramide metabolism in KG-1 and LoVo Cells

We showed that tamoxifen when partnered with C6-ceramide enhanced cytotoxicity and effectively retarded C6-ceramide conversion to C6-GC and C6-SM (see Fig. 5). We hypothesized that the inclusion of tamoxifen would channel more C6-ceramide toward hydrolysis via ceramidase, resulting in liberated sphingosine and an increase in [^{3}H]palmitic acid incorporation into long-chain cellular ceramides. Fig. 7A shows that whereas C6-ceramide and tamoxifen produced approximate 2.1- and 1.8-fold increases in long-chain ^{3}H-ceramide, co-administration resulted in a 9.5-fold increase in long-chain ^{3}H-ceramide. Based on cpm in ^{3}H-ceramide/100,000 cpm total lipid tritium, endogenous ceramide increased from 0.6% of total lipid in control to >6% of the total lipid in KG-1 cells treated with the C6-ceramide/tamoxifen regimen. The addition of unlabeled C6-ceramide enhanced ^{3}H-GC counts by 1.6-fold (Fig. 7B), with tamoxifen displaying a similar effect. Thus, in KG-1 cells exposed to C6-ceramide, long-chain ^{3}H-ceramide and ^{3}H-GC levels increase, representing ceramide synthesis with subsequent glycosylation. However, the C6-ceramide/tamoxifen mix enhanced synthesis of ^{3}H-GC by only 1.2-fold over either agent alone. Therefore, although the C6-ceramide/tamoxifen combination increased ^{3}H-ceramide levels 9.5-fold, the results suggest that cells do not efficiently convert ^{3}H-ceramide to ^{3}H-GC with tamoxifen present. The addition of unlabeled C6-ceramide reduced long-chain ^{3}H-SM synthesis by 56% (Fig. 7C), whereas tamoxifen alone was without influence on ^{3}H-SM synthesis from [^{3}H]palmitate. The tamoxifen/C6-ceramide combination did not alter ^{3}H-SM synthesis over C6-ceramide only. Because tamoxifen redirected C6-ceramide anabolism from C6-GC to C6-SM in LoVo colorectal cancer cells (see Fig. 4), we wanted to determine whether tamoxifen would induce an increase in long-chain ceramides in LoVo cells, as observed in KG-1 cells (Fig. 7A). The data in Fig. 7D show that addition of C6-ceramide produced a slight increase in long-chain ^{3}H-ceramide (1.3-fold), whereas tamoxifen was essentially without influence. The mixture of C6-ceramide and tamoxifen produced a 3.4-fold increase in long-chain ^{3}H-ceramide. While

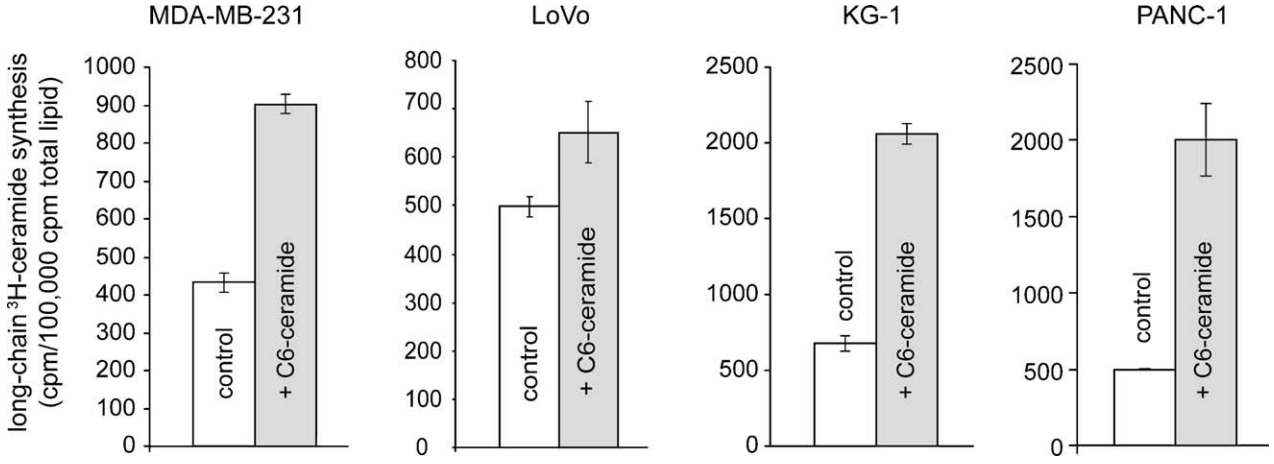

Fig. 6. Effect of C6-ceramide on incorporation of [^{3}H]palmitic acid into long-chain ceramides in human cancer cells. Cells were seeded in 6-well plates (MDA-MB-231 at 5×10^5 cells/well, LoVo at 7.5×10^5 cells/well, KG-1 at 1×10^6 cells/well; PANC-1 at 2×10^5 cells/well) and treated the following day without or with C6-ceramide (10 μM for MDA-MB-231, LoVo, and KG-1, and 12.6 μM for PANC-1) in medium containing 1.0 μCi/ml [^{3}H]palmitic acid for 24 h. Long-chain ^{3}H-ceramides were measured in the total lipid extracts by TLC and LSC.

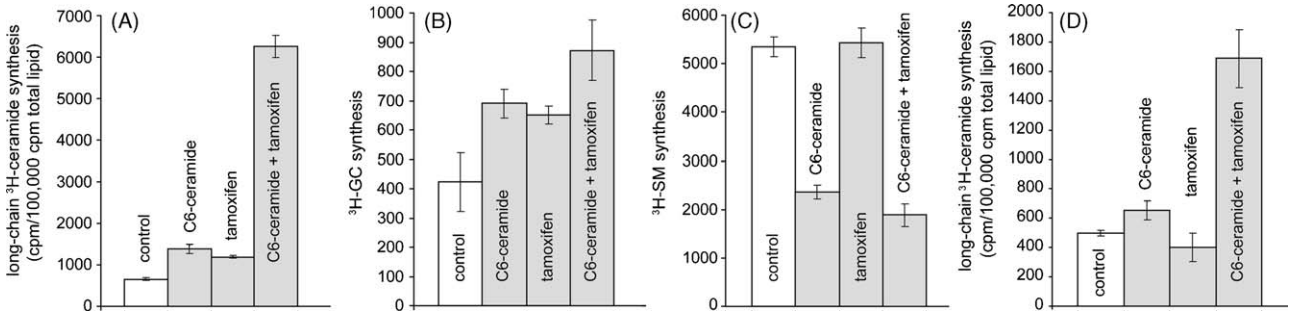

Fig. 7. Influence of tamoxifen on synthesis of long-chain ceramides from C6-ceramide in KG-1 and LoVo cells. Cells were seeded in 6-well plates (KG-1, 1×10^6/well; LoVo, 5×10^5/well) and treated the next day as indicated for 24 h in medium containing [^{3}H]palmitic acid, 1.0 μCi/ml. Concentrations of C6-ceramide and tamoxifen were 10 and 5 μM, respectively. (A–C) Long-chain ^{3}H-ceramide, ^{3}H-GC, and ^{3}H-SM synthesis in KG-1 cells. (D) Long-chain ^{3}H-ceramide synthesis in LoVo cells.

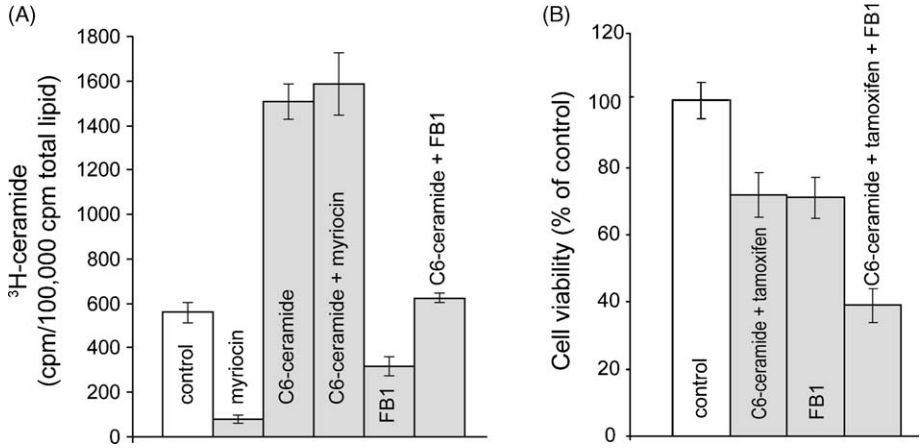

Fig. 8. Effect of ceramide synthesis inhibitors myriocin and FB1 on formation of long-chain ceramides from C6-ceramide and influence on viability in C6-ceramide/tamoxifen-treated KG-1 cells. (A) Effect of inhibition on ^{3}H-ceramide synthesis. Cells (1×10^6/well) were seeded into 6-well plates and treated the next day with either vehicle (ethanol control), myriocin (0.25 μM), C6-ceramide (10 μM), or FB1 (25 μM), or combinations as indicated, in medium containing [^{3}H]palmitic acid (1.0 μCi/ml) for 24 h. ^{3}H-Ceramides were quantitated in the total lipid extract by TLC and LSC. (B) Effect of FB1 on cytotoxicity imparted by C6-ceramide/tamoxifen. Cells were exposed to C6-ceramide/tamoxifen mix (10 μM + 5 μM, respectively) and FB1 (25 μM) for 24 h, the time frame in panel A. Cell viability was measured by MTS.

this effect was not as large as in KG-1 cells, blocking glycosylation with tamoxifen as well resulted in enhanced synthesis of long-chain ceramide in LoVo colorectal cancer cells.

In order to determine whether C6-ceramide stimulated incorporation of [^{3}H]palmitic acid into long-chain ceramide by activation of *de novo* synthesis we tested the effect of inhibitors of *de novo* synthesis. Myriocin is an inhibitor of serine palmitoyltransferase, the first step in ceramide biosynthesis, and fumonisin B1 is an inhibitor of ceramide synthase, which transfers palmitate from palmitoyl CoA to sphingoid base, in this case sphingosine. The results of the experiment in Fig. 8A, in which [^{3}H]palmitic acid was used as a tracer, show that myriocin was an effective inhibitor (86%) of *de novo* ceramide synthesis (compare control to myriocin). C6-ceramide addition increased long-chain ^{3}H-ceramide synthesis by 2.7-fold over control. The increase in ^{3}H-ceramide was not affected by addition of myriocin; however, fumonisin B1 nearly totally blocked the increase in long-chain ^{3}H-ceramide produced when C6-ceramide was present. In both KG-1 and LoVo cells, tamoxifen enhanced the synthesis of ^{3}H-ceramide, perhaps by augmenting the flow of C6-ceramide in the direction of hydrolysis, via ceramidase. This would increase intracellular levels of sphingosine a substrate for ceramide synthase (and sphingosine kinase). As shown in Fig. 8B, we were unable to rescue KG-1 cells from C6-ceramide/tamoxifen cytotoxicity using fumonisin B1, which blocks acylation of sphingosine to long-chain ceramide.

4. Discussion

This study demonstrates the versatility of cancer cells to convert C6-ceramide to higher sphingolipids by GCS and SM synthase, and to hydrolyze C6-ceramide to the component sphingoid base by the action of ceramidase. An early study by Abe et al. [28] demonstrated catabolic and anabolic pathways for octanoyl sphingosine in Madin–Darby canine kidney cells. We previously showed, using various breast cancer cell lines, that high-dose C6-ceramide was primarily converted to C6-GC [29]. Here we demonstrate for the first time that different types of cancer cells metabolize C6-ceramide differently, that the route of metabolism can be dictated by the dose administered, and that tamoxifen, through its capacity to block sphingolipid metabolism, is an effective enhancer of C6-cearmide cytotoxicity. Knowledge of ceramide metabolism in cancer cells can be utilized to augment ceramide-driven cell death cascades. Chan et al. [30] reported in MDA-MB-435 human breast cancer cells that co-administration of either a GCS inhibitor or a ceramidase inhibitor increased the cytotoxic effect of C6-ceramide. Based on metabolic routes, one or a combination of enzyme inhibitors could be employed to enhance efficacy.

The majority of studies on enhancement of ceramide-induced apoptosis have focused on targeting GCS [31,32]. However, the capacity of P-gp antagonists to block GC synthesis [14,15] makes

these drugs attractive as partnering agents with short-chain ceramides and ceramide-generating compounds. Our studies on C6-ceramide metabolism led us to investigate whether tamoxifen would enhance cytotoxic effect. Here we show that C6-ceramide/tamoxifen was an effective regimen for inducing cell death in several types of cultured tumor cells. Whereas agents like PPMP and the imido sugars [29] inhibit GCS, P-gp antagonists block GC synthesis by limiting glycolipid trafficking at the Golgi. It has been shown that P-gp can act as a flipase for glycosphingolipids including GC [33]; however, it should be noted that nitrobenzo-2-oxa-1, 3-diazole-labled lipids were used in those experiments. Other types of ABC transporters as well demonstrate specificity for lipid translocation [34,35].

Tamoxifen effectively inhibited synthesis of C6-GC from C6-ceramide in MDA-MB-231, LoVo, and KG-1 cells, but demonstrated a cell-specific influence on C6-SM metabolism. In KG-1 leukemia cells in which drug synergy was most marked, tamoxifen inhibited both C6-GC and C6-SM synthesis (see Fig. 5). In LoVo cells tamoxifen blocked C6-GC formation and redirected C6-ceramide toward C6-SM synthesis. This indicates increased anabolism of C6-ceramide in LoVo cells and increased hydrolysis as marked by the generation of long-chain ceramides. Thus in final analysis it would appear that C6-ceramide levels are very low in tamoxifen-treated LoVo cells. These novel effects and the potent cytotoxic response led us to explore further the mechanism of action of C6-ceramide/tamoxifen.

Modulation of apoptosis by C6-ceramide is likely governed by several lipid factors. Although C6-ceramide itself can induce cell death, Takeda et al. [36] demonstrated in keratinocytes that apoptosis occurred via a ceramide recycling pathway, whereby sphingosine from hydrolyzed C6-ceramide was reacylated in long-chain ceramide. Ogretmen et al. [27] also demonstrated in A549 lung adenocarcinoma cells that generation of endogenous ceramide in response to C6-ceramide supplements was due to recycling of the sphingosine backbone of C6-ceramide. Our experiments support these findings, as we showed that the inclusion of unlabeled C6-ceramide with [^{3}H]palmitic acid (the acyl chain source for ceramide synthase) increased by 3-fold the synthesis of long-chain ^{3}H-ceramides in KG-1 cells. Similar trends were also observed in MDA-MB-231, and PANC-1 and LoVo cells. With the curious property of tamoxifen to block both GC and SM synthesis in KG-1 cells, we hypothesized that in cells exposed to tamoxifen, intracellular C6-ceramide would be channeled toward hydrolysis. Indeed, whereas unlabeled C6-ceramide produced an approximate 2.1-fold increase in ^{3}H-ceramides, adding tamoxifen with C6-ceramide resulted in a 9.5-fold increase over control in long-chain ^{3}H-ceramides (see Fig. 7). The experiments using fumonisin B1, an inhibitor of the acyl transferase reaction catalyzed by ceramide synthase, demonstrated a clear involvement of ceramide synthase in the generation of long-chain ceramides from C6-ceramide.

Cultured tumor cells express intracytoplasmic drug transporter proteins such as P-gp [37]. For example, prostate cancer cells were shown to express MRP mRNA and protein before selection with doxorubicin [38]. Similarly, chemotherapy-naïve human melanoma cell lines express Golgi-associated P-gp but not cell-surface P-gp. We propose that intracytoplasmic drug transporter proteins, such as P-gp, can be promising therapeutic targets. We have shown using a Hela cell model with conditional expression of P-gp that the efficacy of tamoxifen for enhancing C6-ceramide cytotoxicity was dependent on the presence of P-gp (unpublished data, author's laboratory).

Combining C6-ceramide with tamoxifen clearly enhanced the cytotoxic impact of either single agent. When used with a (dihydro)ceramide generator such as fenretinide (4-HPR), tamoxifen increased ceramide levels and decreased viability in PC-3 prostate cancer cells to an extent greater than PPMP [39]. In a recent study of ovarian adenocarcinoma, it was shown that tamoxifen-loaded nanoparticles modulated paclitaxel resistance by enhancing intracellular ceramide levels [40]. In another study, tamoxifen combined with 4-HPR inhibited growth of MDA-MB-231 cells, a response the authors attributed to a marked increase in ganglioside GM_3 [41].

Recent interest in ceramide-based therapies necessitates that we have a better understanding of ceramide metabolism, including the exogenously applied, cell-permeable analogs that are currently being investigated using novel delivery systems. In a study of acyl chain length and apoptotic activity, C6-ceramide was found most active, with IC_{50} measurements of 3–14 μM in MDA435/LCC6 breast cancer cells [42]. These investigators also found that intracellular delivery of ceramide via liposomes enhanced apoptosis. Recent investigations with nanoliposomal dispersions of C6-ceramide show that this nanoscale delivery system offers rapid tissue distribution *in vivo* without adverse effects [20], and in allied preclinical studies nanoliposomal ceramide enhanced sorafenib efficacy in melanoma and breast cancer cell models [43]. These studies support use of C6-ceramide/tamoxifen for targeting tumor cells *in vivo*. The addition of tamoxifen to the nanoliposomal formulation could extend efficacy by limiting ceramide clearance through the glycosylation and/or SM synthase pathways. Interestingly, fumonisin B1, which blocks acylation of sphingosine liberated by C6-ceramide hydrolysis, failed to rescue KG-1 cells from C6-ceramide/tamoxifen cytotoxicity. We conclude that the effect of the C6-ceramide/tamoxifen combination on cell viability is not correlated with the formation of long-chain ceramides, but rather with levels of the sphingoid base, sphingosine and with C6-ceramide [44]. However, sensitivity to C6-ceramide and metabolites, sphingosine and long-chain ceramides, may well be cell type-specific.

Acknowledgements

The authors are grateful to Kenneth Baas for constructing the figures. This research was supported by USPHS grants GM77391 and CA143755, the Association for Breast and Prostate Cancer Studies (Los Angeles), and the Fashion Footwear Association of New York Charitable Foundation (New York, NY). We thank Matt Bush for compiling the typescript.

References

[1] Lavie Y, Cao H, Bursten SL, Giuliano AE, Cabot MC. Accumulation of glucosylceramides in multidrug-resistant cancer cells. J Biol Chem 1996;271:19530–6.
[2] Lucci A, Cho WI, Han TY, Giuliano AE, Morton DL, Cabot MC. Glucosylceramide: a marker for multiple-drug resistant cancers. Anticancer Res 1998;18:475–80.
[3] Liu YY, Yu JY, Yin D, Patwardhan GA, Gupta V, Hirabayashi Y, et al. A role for ceramide in driving cancer cell resistance to doxorubicin. FASEB J 2008;22:2541–51.
[4] Kok JW, Veldman RJ, Klappe K, Koning H, Filipeanu CM, Muller M. Differential expression of sphingolipids in MRP1 overexpressing HT29 cells. Int J Cancer 2000;87:172–8.
[5] Gouaze V, Yu JY, Bleicher RJ, Han TY, Liu YY, Wang H, et al. Overexpression of glucosylceramide synthase and P-glycoprotein in cancer cells selected for resistance to natural product chemotherapy. Mol Cancer Ther 2004;3:633–9.
[6] Cabot MC, Giuliano AE. Apoptosis—a cell mechanism important for cytotoxic response to adriamycin and a lipid metabolic pathway that facilitates escape. Breast Cancer Res Treat 1997;47:71.
[7] Liu YY, Han TY, Giuliano AE, Cabot MC. Expression of glucosylceramide synthase, converting ceramide to glucosylceramide, confers adriamycin resistance in human breast cancer cells. J Biol Chem 1999;274:1140–6.
[8] Liu YY, Han TY, Giuliano AE, Hansen N, Cabot MC. Uncoupling ceramide glycosylation by transfection of glucosylceramide synthase antisense reverses adriamycin resistance. J Biol Chem 2000;275:7138–43.
[9] Cabot M. Ceramide glycosylation and chemotherapy resistance. In: Futerman AH, editor. Ceramide signaling. Georgetown, Texas: Landes Bioscience; 2002. p. 133–9.

[10] Lucci A, Giuliano AE, Han TY, Dinur T, Liu YY, Senchenkov A, et al. Ceramide toxicity and metabolism differ in wild-type and multidrug-resistant cancer cells. Int J Oncol 1999;15:535–40.
[11] Liu YY, Han TY, Giuliano AE, Ichikawa S, Hirabayashi Y, Cabot MC. Glycosylation of ceramide potentiates cellular resistance to tumor necrosis factor-alpha-induced apoptosis. Exp Cell Res 1999;252:464–70.
[12] Patwardhan GA, Zhang QJ, Yin D, Gupta V, Bao J, Senkal CE, et al. A new mixed-backbone oligonucleotide against glucosylceramide synthase sensitizes multidrug-resistant tumors to apoptosis. PLoS One 2009;4:e6938.
[13] Gouaze V, Liu YY, Prickett CS, Yu JY, Giuliano AE, Cabot MC. Glucosylceramide synthase blockade down-regulates P-glycoprotein and resensitizes multidrug-resistant breast cancer cells to anticancer drugs. Cancer Res 2005;65:3861–7.
[14] Cabot MC, Giuliano AE, Volner A, Han TY. Tamoxifen retards glycosphingolipid metabolism in human cancer cells. FEBS Lett 1996;394:129–31.
[15] Lavie Y, Cao H, Volner A, Lucci A, Han TY, Geffen V, et al. Agents that reverse multidrug resistance, tamoxifen, verapamil, and cyclosporin A, block glycosphingolipid metabolism by inhibiting ceramide glycosylation in human cancer cells. J Biol Chem 1997;272:1682–7.
[16] Abe A, Inokuchi J, Jimbo M, Shimeno H, Nagamatsu A, Shayman JA, et al. Improved inhibitors of glucosylceramide synthase. J Biochem 1992;111:191–6.
[17] Sietsma H, Veldman RJ, Kolk D, Ausema B, Nijhof W, Kamps W, et al. 1-phenyl-2-decanoylamino-3-morpholino-1-propanol chemosensitizes neuroblastoma cells for taxol and vincristine. Clin Cancer Res 2000;6:348–942.
[18] Spinedi A, Bartolomeo SD, Piacentini M. Apoptosis induced by N-hexanoyl-sphingosine in CHP-100 cells associates with accumulation of endogenous ceramide and is potentiated by inhibition of glucocerebroside synthesis. Cell Death Differ 1998;5:785–91.
[19] Reynolds CP, Frgala T, Tsao-Wie DD, Groshen S, Morgan R, McNamara M, et al. High plasma levels of fenretinide (4-HPR) were associated with improved outcome in a phase II study of recurrent ovarian cancer: a study by the California Cancer Consortium ASCO. Chicago, IL; 2007. p. 287S.
[20] Zolnik BS, Stern ST, Kaiser JM, Heakal Y, Clogston JD, Kester M, et al. Rapid distribution of liposomal short-chain ceramide in vitro and in vivo. Drug Metab Dispos 2008;36:1709–15.
[21] Senchenkov A, Litvak DA, Cabot MC. Targeting ceramide metabolism—a strategy for overcoming drug resistance. J Natl Cancer Inst 2001;93:347–57.
[22] Van Brocklyn JR. Sphingolipid signaling pathways as potential therapeutic targets in gliomas. Mini Rev Med Chem 2007;7:984–90.
[23] Shida D, Takabe K, Kapitonov D, Milstien S, Spiegel S. Targeting SphK1 as a new strategy against cancer. Curr Drug Targets 2008;9:662–73.
[24] Lamour NF, Chalfant CE. Ceramide kinase and the ceramide-1-phosphate/cPLA2alpha interaction as a therapeutic target. Curr Drug Targets 2008;9:674–82.
[25] Saddoughi SA, Song P, Ogretmen B. Roles of bioactive sphingolipids in cancer biology and therapeutics. Subcell Biochem 2008;49:413–40.
[26] Bielawska a, Hannun YA. Radiolabeled sphigolipids. Part II. Preparation of radiolabeled ceramides and phosphoingolipids. In: Merrill AH, Hannun YA, editors. Methods in enzymology: sphingolipid metabolism and cell signaling, Parts A and B. San Diego: Academic Press; 2000. p. 499–518.
[27] Ogretmen B, Pettus BJ, Rossi MJ, Wood R, Usta J, Szulc Z, et al. Biochemical mechanisms of the generation of endogenous long chain ceramide in response to exogenous short chain ceramide in the A549 human lung adenocarcinoma cell line. Role for endogenous ceramide in mediating the action of exogenous ceramide. J Biol Chem 2002;277:12960–9.
[28] Abe A, Wu D, Shayman JA, Radin NS. Metabolic effects of short-chain ceramide and glucosylceramide on sphingolipids and protein kinase C. Eur J Biochem 1992;210:765–73.
[29] Andersson U, Butters TD, Dwek RA, Platt FM. N-butyldeoxygalactonojirimycin: a more selective inhibitor of glycosphingolipid biosynthesis than N-butyldeoxynojirimycin, in vitro and in vivo. Biochem Pharmacol 2000;59:821–9.
[30] Chan SY, Hilchie AL, Brown MG, Anderson R, Hoskin DW. Apoptosis induced by intracellular ceramide accumulation in MDA-MB-435 breast carcinoma cells is dependent on the generation of reactive oxygen species. Exp Mol Pathol 2007;82:1–11.
[31] Bleicher RJ, Cabot MC. Glucosylceramide synthase and apoptosis. Biochim Biophys Acta 2002;1585:172–8.
[32] Gouaze-Andersson V, Cabot MC. Glycosphingolipids and drug resistance. Biochim Biophys Acta 2006;1758:2096–103.
[33] Eckford PD, Sharom FJ. The reconstituted P-glycoprotein multidrug transporter is a flippase for glucosylceramide and other simple glycosphingolipids. Biochem J 2005;389:517–26.
[34] Borst P, Zelcer N, van Helvoort A. ABC transporters in lipid transport. Biochim Biophys Acta 2000;1486:128–44.
[35] van Helvoort A, Smith AJ, Sprong H, Fritzsche I, Schinkel AH, Borst P, et al. MDR1 P-glycoprotein is a lipid translocase of broad specificity, while MDR3 P-glycoprotein specifically translocates phosphatidylcholine. Cell 1996;87:507–17.
[36] Takeda S, Mitsutake S, Tsuji K, Igarashi Y. Apoptosis occurs via the ceramide recycling pathway in human HaCaT keratinocytes. J Biochem 2006;139:255–62.
[37] Molinari A, Calcabrini A, Meschini S, Stringaro A, Crateri P, Toccacieli L, et al. Subcellular detection and localization of the drug transporter P-glycoprotein in cultured tumor cells. Curr Protein Pept Sci 2002;3:653–70.
[38] David-Beabes GL, Overman MJ, Petrofski JA, Campbell PA, de Marzo AM, Nelson WG. Doxorubicin-resistant variants of human prostate cancer cell lines DU 145, PC-3, PPC-1, and TSU-PR1: characterization of biochemical determinants of antineoplastic drug sensitivity. Int J Oncol 2000;17:1077–86.
[39] Wang H, Charles AG, Frankel AJ, Cabot MC. Increasing intracellular ceramide: an approach that enhances the cytotoxic response in prostate cancer cells. Urology 2003;61:1047–52.
[40] Devalapally H, Duan Z, Seiden MV, Amiji MM. Modulation of drug resistance in ovarian adenocarcinoma by enhancing intracellular ceramide using tamoxifen-loaded biodegradable polymeric nanoparticles. Clin Cancer Res 2008;14:3193–203.
[41] Aoyama C, Ohtani A, Ishidate K. Expression and characterization of the active molecular forms of choline/ethanolamine kinase-alpha and -beta in mouse tissues, including carbon tetrachloride-induced liver. Biochem J 2002;363:777–84.
[42] Shabbits JA, Mayer LD. Intracellular delivery of ceramide lipids via liposomes enhances apoptosis in vitro. Biochim Biophys Acta 2003;1612:98–106.
[43] Tran MA, Smith CD, Kester M, Robertson GP. Combining nanoliposomal ceramide with sorafenib synergistically inhibits melanoma and breast cancer cell survival to decrease tumor development. Clin Cancer Res 2008;14:3571–81.
[44] Wang H, Maurer BJ, Liu YY, Wang E, Allegood JC, Kelly S, et al. N-(4-Hydroxyphenyl)retinamide increases dihydroceramide and synergizes with dimethylsphingosine to enhance cancer cell killing. Mol Cancer Ther 2008;7:2967–76.